

## Supporting Information

One-step integration of amorphous RuBx and crystalline Ru nanoparticles into N-doped porous carbon polyhedrals for robust electrocatalytic activity towards HER in both acidic and basic media

*Jie Tang, Biao Wang, Yanzheng Zhang, Xiaohua Zhang\*, Qinghui Shen, Junfeng Qin, Song Xue, Xi Guo, Cuicui Du\* and Jinhua Chen\**

State Key Laboratory of Chemo/Biosensing and Chemometrics, Advanced Catalytic Engineering Research Center of the Ministry of Education, Provincial Hunan Key Laboratory for Cost-effective Utilization of Fossil Fuel Aimed at Reducing Carbon-dioxide Emissions, College of Chemistry and Chemical Engineering, Hunan University, Changsha, 410082, P.R. China.

---

\* Corresponding author. Tel.: +86-731-88821848

E-mail address: mickyxie@hnu.edu.cn (X. H. Zhang), ducc@hnu.edu.cn (C. C. Du), chenjinhua@hnu.edu.cn (J. H. Chen).

**Contents:**

**Supplementary 1. TEM images for a) ZIF-8 and b) NPCH**

**Supplementary 2. N<sub>2</sub> adsorption-desorption isotherm (a) and pore size distribution curves (b) for NPCH, RuB<sub>x</sub>-Ru@BNPCH and Ru@NPCH**

**Supplementary 3. XRD patterns of ZIF-8, NPCH, RuB<sub>x</sub>-Ru@BNPCH and Ru@NPCH**

**Supplementary 4. EELS spectra of RuB<sub>x</sub>-Ru@BNPCH (the insets are schematic for EELS acquisition regions and the points for a and b from amorphous particles and crystalline particles, respectively, which were obtained by STEM)**

**Supplementary 5. Comparison of HER catalytic activity between RuB<sub>x</sub>-Ru@BNPCH product and other well-developed Ru-based and Transition metal boride based HER electrocatalysts in 1.0 M KOH solution**

**Supplementary 6. LSV curves of RuB<sub>x</sub>-Ru@BNPCH with the mass of Ru in 1M KOH and (b) histogram of mass activity at different overpotentials**

**Supplementary 7. Cyclic voltammetry tests in a non-Faradaic region (0.46 to 0.66 V vs RHE) with different scan rates to determine the electrochemical double layer capacitance C<sub>dl</sub>: the RuB<sub>x</sub>-Ru@BNPCH (a) and Ru@NPCH (b) in 1.0 M KOH**

**Supplementary 8. Comparison of HER catalytic activity between RuB<sub>x</sub>-Ru@BNPCH product and other well-developed Ru-based and Transition metal boride based HER electrocatalysts in 0.5 M H<sub>2</sub>SO<sub>4</sub> solution**

**Supplementary 9. TEM a) and HRTEM b) images for RuB<sub>x</sub>-Ru@BNPCH after the CV cycling test**

Supplementary 10. Polarization curves of RuB<sub>x</sub>-Ru@BNPCH for several batches of samples with the same method

Supplementary 11. (a) LSV curves of water electrolysis for RuB<sub>x</sub>-Ru@BNPCH//RuO<sub>2</sub> and commercial Pt/C//RuO<sub>2</sub> at a scan rate of 5 mV s<sup>-1</sup> in 1 M KOH, (b) Chronoamperometric curve for water electrolysis with constant current density of 10 mA cm<sup>-2</sup> for RuB<sub>x</sub>-Ru@BNPCH//RuO<sub>2</sub> in 1 M KOH.

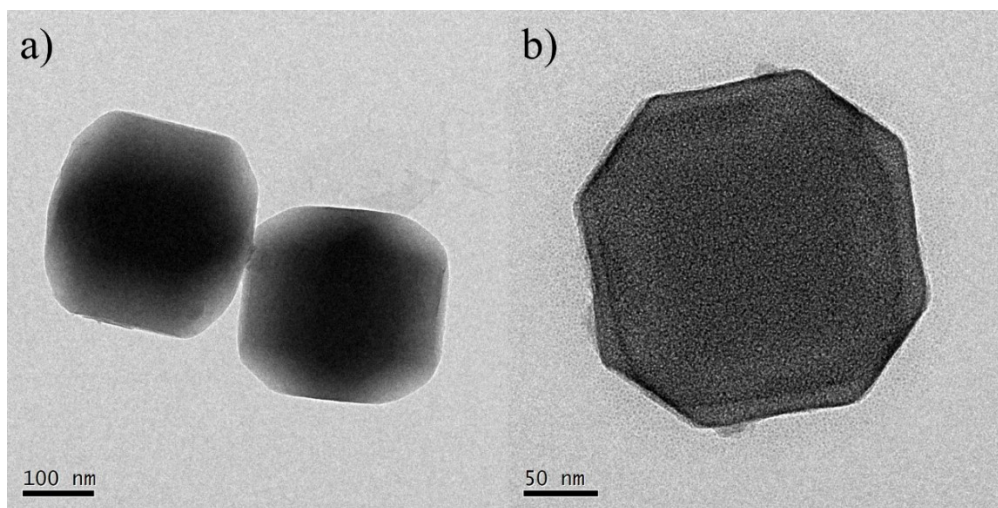
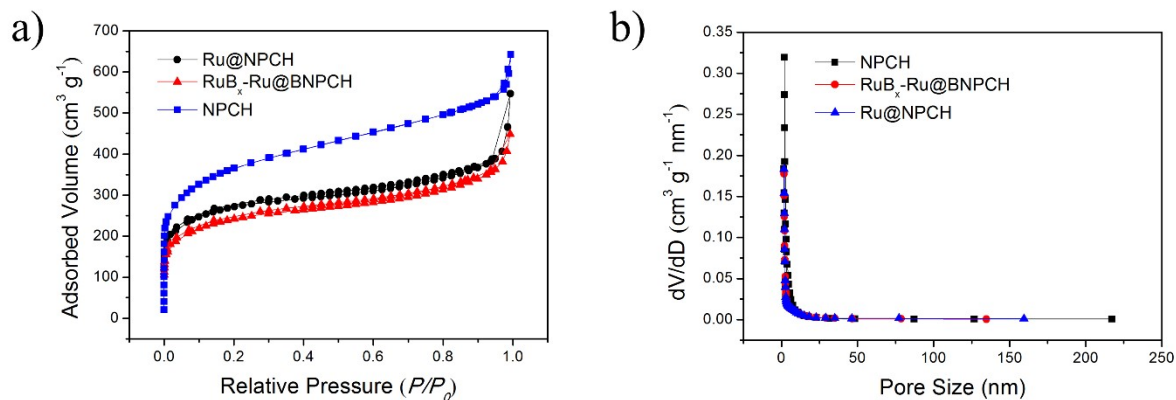
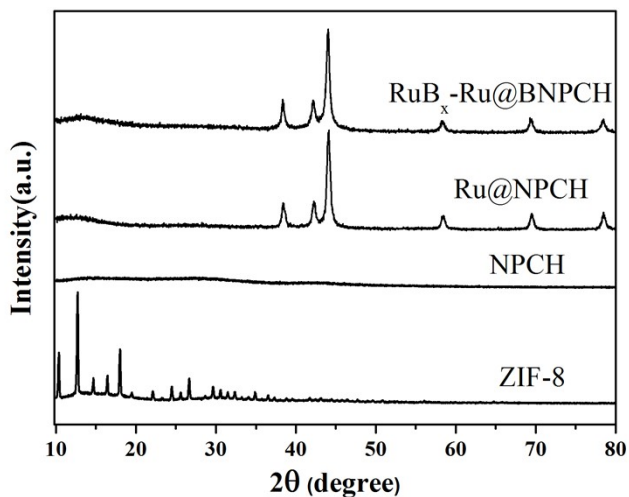


Figure S1. TEM images for a) ZIF-8 and b) NPCH



**Figure S2.** N<sub>2</sub> adsorption-desorption isotherm (a) and pore size distribution curves (b) for NPCH, RuB<sub>x</sub>-Ru@BNPCH and Ru@NPCH



**Figure S3.** XRD patterns of ZIF-8, NPCH, RuB<sub>x</sub>-Ru@BNPCH and Ru@NPCH

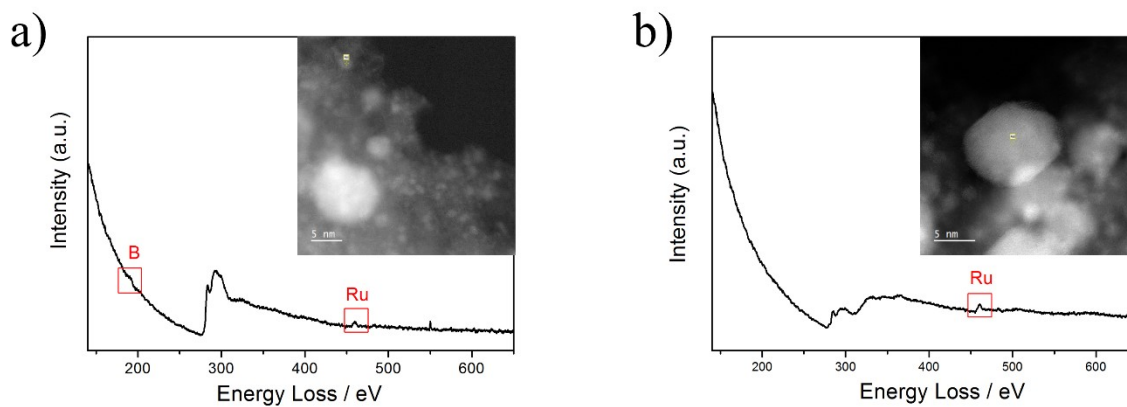


**Figure S4.** EELS spectra of RuB<sub>x</sub>-Ru@BNPCH (the insets are schematic for EELS acquisition regions and the points for a and b from amorphous particles and crystalline particles, respectively, which were obtained by STEM).

**Table S1** Comparison of HER catalytic activity between RuB<sub>x</sub>-Ru@BNPCH product and other well-developed Ru-based and Transition metal boride based HER electrocatalysts in 1.0 M KOH solution.

Catalysts	$E_{(j=10\text{mA cm}^{-2})}$ (mV)	Tafel slope (mV dec <sup>-1</sup> )	Reference
RuB <sub>x</sub> -Ru@BNPCH	5	22.2	<b>This work</b>
Pt/C	22	48.9	1
Ru <sub>2</sub> B <sub>3</sub> @BNC	14	53.9	1
RuB <sub>2</sub>	28	28.7	2
Ru NCs/BNG	14	28.9	3
Ru <sub>2</sub> B <sub>3</sub>	14.6	27.3	4
RuSe <sub>2</sub>	29.5	39.2	5
RuIrO <sub>x</sub>	13	23	6
3D RuCu NCs	18	59	7
RuP <sub>2</sub> @NPC	52	69	8
Co <sub>2</sub> B-500/NG	127	92.4	9
FeB <sub>2</sub>	61	87.5	10
Co-50Ni-B/CC	80	88.2	11
Co-B-P/NF	42	42.1	12

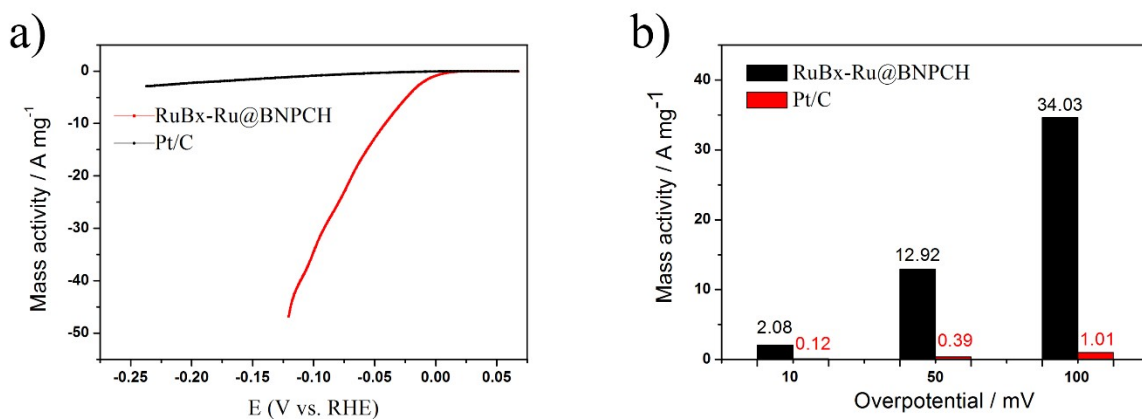


**Figure S5.** LSV curves of RuBx-Ru@BNPCH with the mass of Ru in 1M KOH and (b) histogram of mass activity at different overpotentials

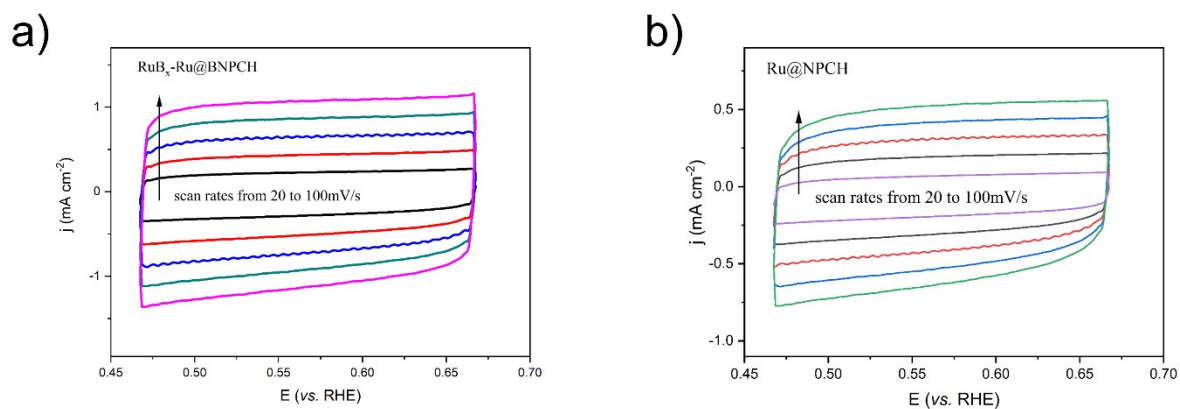


**Figure S6.** Cyclic voltammetry tests in a non-Faradaic region (0.46 to 0.66 V vs RHE) with different scan rates to determine the electrochemical double layer capacitance  $C_{dl}$ : the RuBx-Ru@BNPCH (a) and Ru@NPCH (b) in 1.0 M KOH.

**Table S2.** Comparison of HER catalytic activity between RuB<sub>x</sub>-Ru@BNPCH product and other well-developed Ru-based and Transition metal boride based HER electrocatalysts in 0.5 M H<sub>2</sub>SO<sub>4</sub> solution.

Catalysts	$E_{(j=10\text{mA cm}^{-2})}$ (mV)	Tafel slope (mV dec <sup>-1</sup> )	Reference
RuB <sub>x</sub> -Ru@BNPCH	33	37.8	<b>This work</b>
Ru <sub>2</sub> B <sub>3</sub> @BNC	41	60.7	1
RuTe <sub>2</sub> -M	35.7	46.6	5
RuP <sub>2</sub> @NPC	38	38	8
RuB <sub>2</sub>	52	66.9	13
Pt/C	34	31.2	13
RuP@NPC	51	46	14
RuP-475	47	39	15
α-MoB <sub>2</sub>	120	74.2	16
Ni <sub>3</sub> B	79	85.32	17

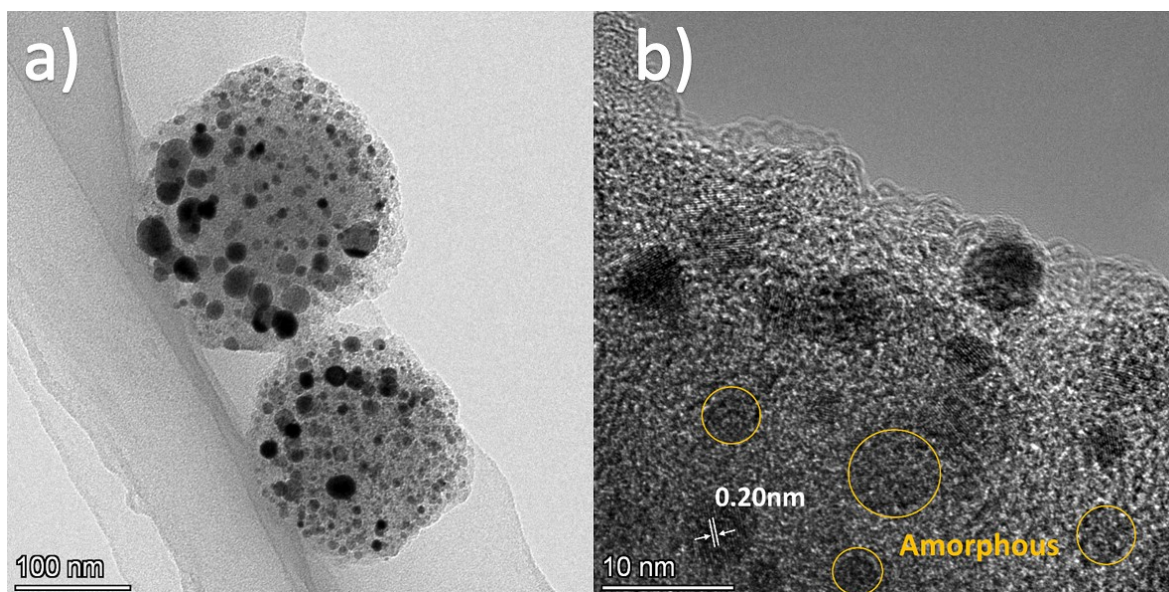


**Figure S7.** TEM a) and HRTEM b) images for RuBx-Ru@BNPCH after the CV cycling test

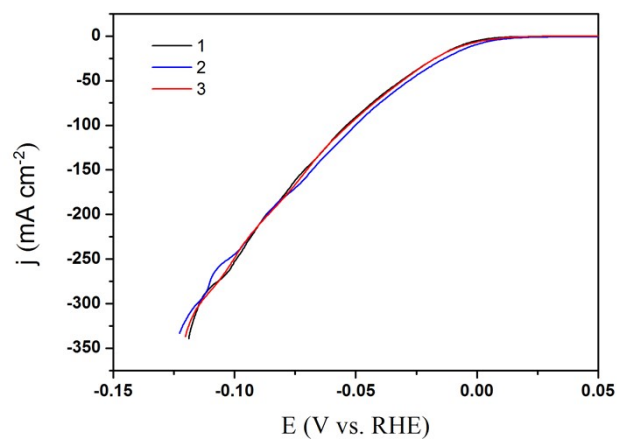


**Figure S8.** Polarization curves of RuBx-Ru@BNPCH for several batches of samples with the same method

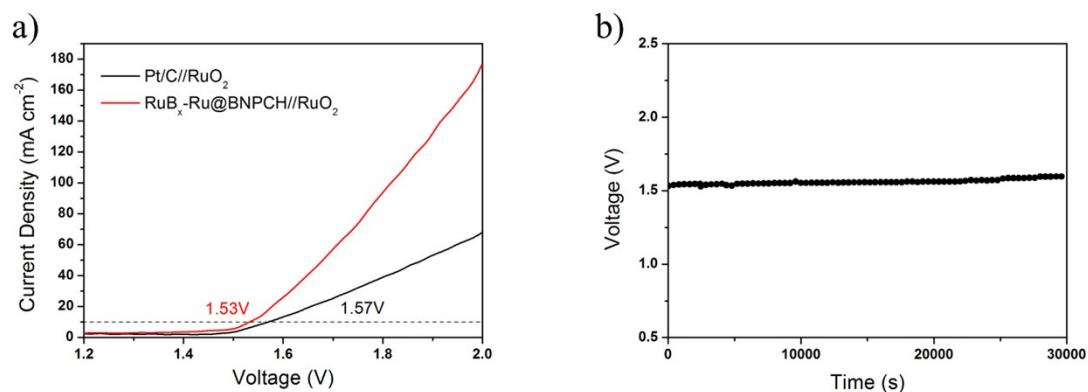


**Figure S9.** (a) LSV curves of water electrolysis for RuB<sub>x</sub>-Ru@BNPCH//RuO<sub>2</sub> and commercial Pt/C//RuO<sub>2</sub> at a scan rate of 5 mV s<sup>-1</sup> in 1 M KOH, (b) Chronoamperometric curve for water electrolysis with constant current density of 10 mA cm<sup>-2</sup> for RuB<sub>x</sub>-Ru@BNPCH//RuO<sub>2</sub> in 1 M KOH.

## Reference

1. Y. Qiao, P. Yuan, C.-W. Pao, Y. Cheng, Z. Pu, Q. Xu, S. Mu and J. Zhang, *Nano Energy*, 2020, **75**, 104881.
2. Q. Li, X. Zou, X. Ai, H. Chen, L. Sun and X. Zou, *Advanced Energy Materials*, 2018, DOI: 10.1002/aenm.201803369, 1803369.
3. S. Ye, F. Luo, T. Xu, P. Zhang, H. Shi, S. Qin, J. Wu, C. He, X. Ouyang, Q. Zhang, J. Liu and X. Sun, *Nano Energy*, 2020, **68**, 104301.
4. X. Zou, L. Wang, X. Ai, H. Chen and X. Zou, *Chemical communications*, 2020, **56**, 3061-3064.
5. Z. Zhang, C. Jiang, P. Li, K. Yao, Z. Zhao, J. Fan, H. Li and H. Wang, *Small*, 2021, **17**, e2007333.
6. Z. Zhuang, Y. Wang, C. Q. Xu, S. Liu, C. Chen, Q. Peng, Z. Zhuang, H. Xiao, Y. Pan, S. Lu, R. Yu, W. C. Cheong, X. Cao, K. Wu, K. Sun, Y. Wang, D. Wang, J. Li and Y. Li, *Nature communications*, 2019, **10**, 4875.
7. D. Cao, J. Wang, H. Xu and D. Cheng, *Small*, 2020, **16**, 2000924.
8. Z. Pu, I. S. Amiinu, Z. Kou, W. Li and S. Mu, *Angewandte Chemie International Edition*, 2017, **56**, 11559-11564.
9. J. Masa, P. Weide, D. Peeters, I. Sinev, W. Xia, Z. Sun, C. Somsen, M. Muhler and W. Schuhmann, *Advanced Energy Materials*, 2016, **6**, 1502313.
10. H. Li, P. Wen, Q. Li, C. Dun, J. Xing, C. Lu, S. Adhikari, L. Jiang, D. L. Carroll and S. M. Geyer, *Advanced Energy Materials*, 2017, **7**, 1700513.
11. M. Sheng, Q. Wu, Y. Wang, F. Liao, Q. Zhou, J. Hou and W. Weng, *Electrochemistry Communications*, 2018, **93**, 104-108.

12. H. Sun, X. Xu, Z. Yan, X. Chen, L. Jiao, F. Cheng and J. Chen, *Journal of Materials Chemistry A*, 2018, **6**, 22062-22069.
13. D. Chen, T. Liu, P. Wang, J. Zhao, C. Zhang, R. Cheng, W. Li, P. Ji, Z. Pu and S. Mu, *ACS Energy Letters*, 2020, **5**, 2909-2915.
14. J.-Q. Chi, W.-K. Gao, J.-H. Lin, B. Dong, K.-L. Yan, J.-F. Qin, B. Liu, Y.-M. Chai and C.-G. Liu, *ChemSusChem*, 2018, **11**, 743-752.
15. Q. Chang, J. Ma, Y. Zhu, Z. Li, D. Xu, X. Duan, W. Peng, Y. Li, G. Zhang, F. Zhang and X. Fan, *ACS Sustainable Chemistry & Engineering*, 2018, **6**, 6388-6394.
16. Y. Chen, G. Yu, W. Chen, Y. Liu, G. D. Li, P. Zhu, Q. Tao, Q. Li, J. Liu, X. Shen, H. Li, X. Huang, D. Wang, T. Asefa and X. Zou, *Journal of the American Chemical Society*, 2017, **139**, 12370-12373.
17. X. Xu, Y. Deng, M. Gu, B. Sun, Z. Liang, Y. Xue, Y. Guo, J. Tian and H. Cui, *Applied Surface Science*, 2019, **470**, 591-595.